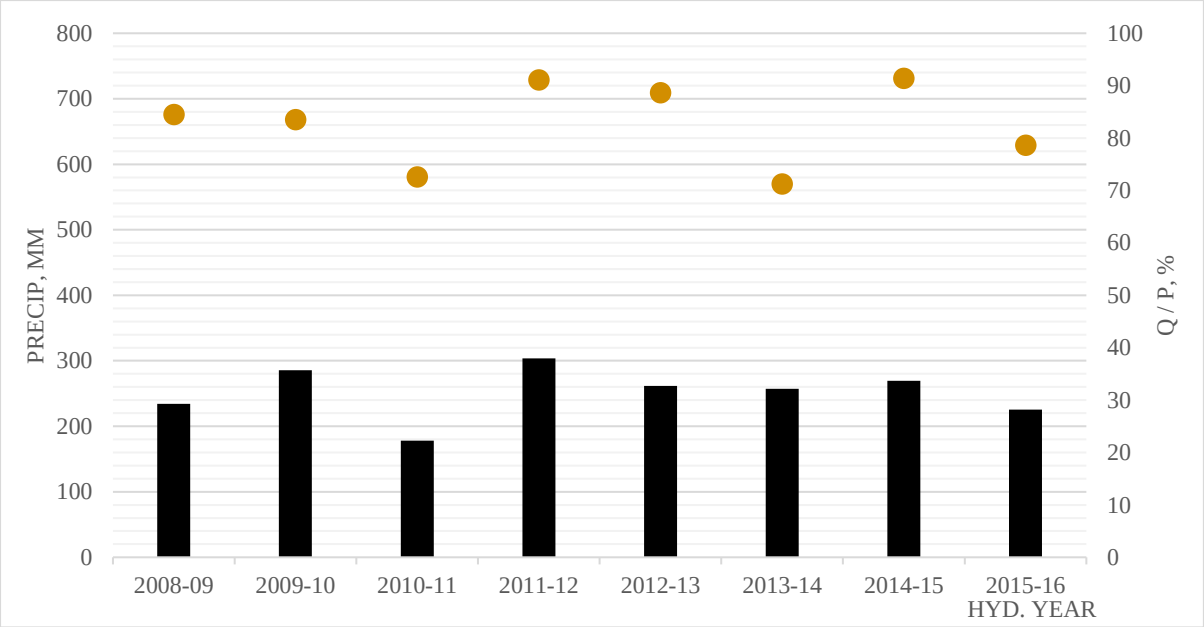

Figure S1. Annual precipitation (dots) and Q/P fraction (bars) over 8 hydrological years for the catchment C2.

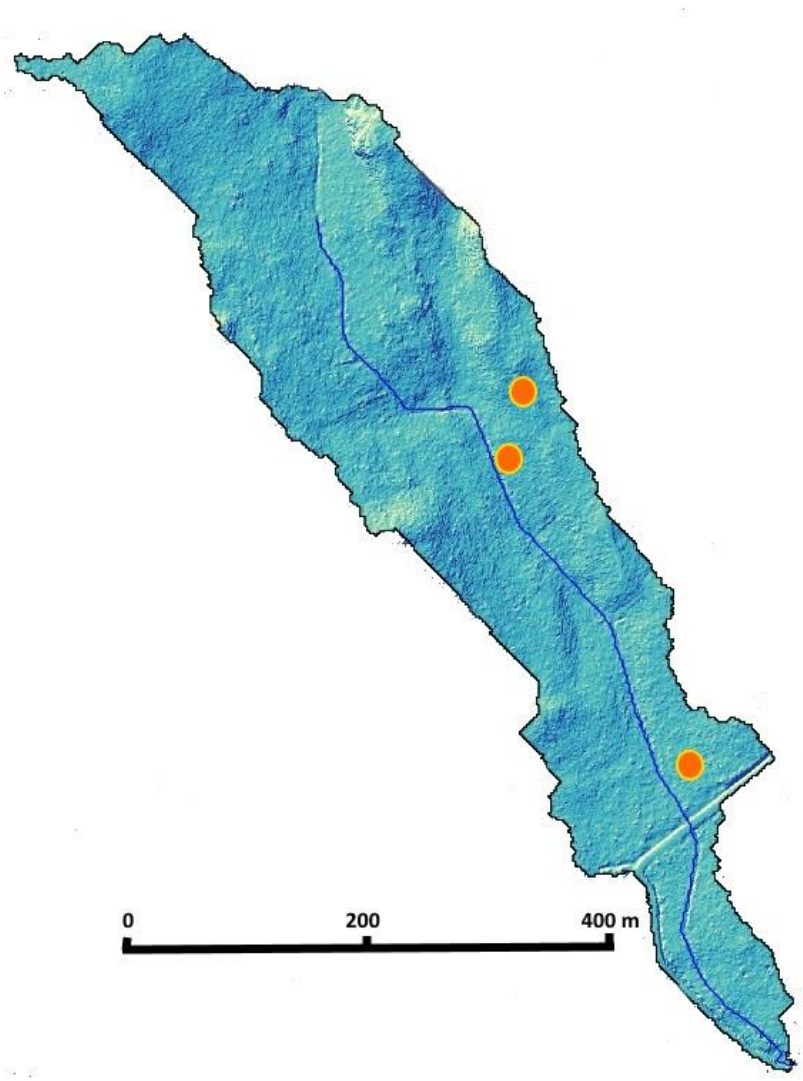

Figure S2. Locations of three nodes of the sap flow measurements within a subcatchment C2.

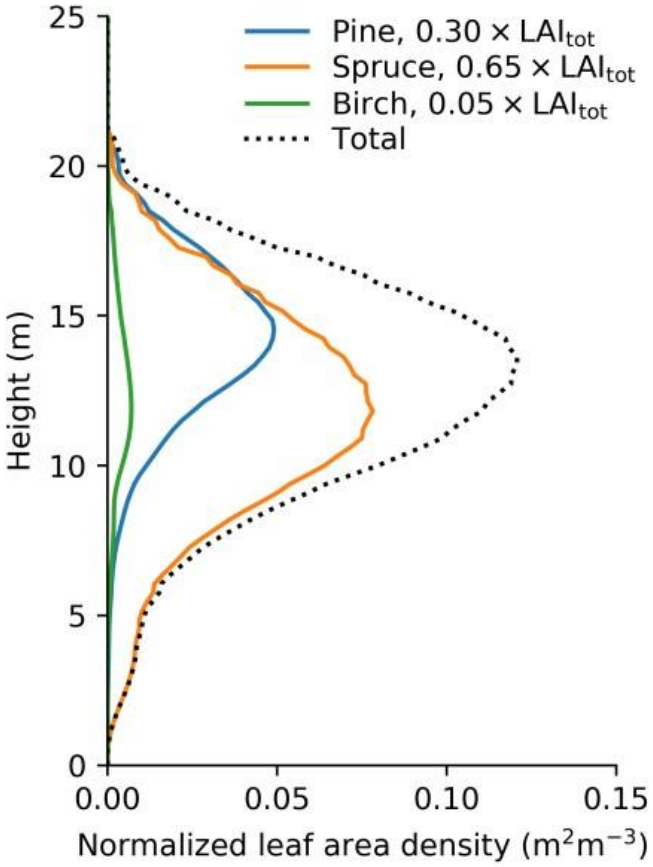

Figure S3. Normalized leaf area density distributions for main tree species and their fraction of total stand leaf area index (LAI_{tot}) at subcatchment C2.

Table S1. Model parameter values applied in simulations (for plant type specific parameters see Table S2).

Description	Parameter value	Source
Canopy radiation parameters		
Clumping coefficient (-)	0.7	(Campbell and Norman, 1998)
Leaf-angle distribution (-)	1.0 (spherical)	(Campbell and Norman, 1998)
Shoot PAR albedo (-)	0.1	Adjusted to match canopy albedo
Shoot NIR albedo (-)	0.39	Adjusted to match canopy albedo
Leaf emissivity (-)	0.98	(Campbell and Norman, 1998)
Canopy flow parameters		
Normalized horizontal pressure gradient (m s^{-2})	0.01	
Foliage drag coefficient (-)	0.15	(Lee et al., 1994)
Schmidt number for H_20, T, CO_2	2.0	
Canopy interception parameters		
Maximum interception storage (mm)	0.2–0.5 × LAI	(Watanabe and Mizutani, 1996)
Leaf orientation factor (-)	0.5 (random)	(Watanabe and Mizutani, 1996)
Plant type parameters for photosynthesis–stomatal conductance model		
Carboxylation capacity V_{cmax} at 25°C (µmol m^{-2} s^{-1})[a]	V_{cmax25}	see Table 2
Electron transport capacity J_{max} at 25°C (µmol m^{-2} s^{-1})[a]	1.97 × V_{cmax25}	(Kattge and Knorr, 2007)
Leaf dark respiration rate r_d at 25°C (µmol m^{-2} s^{-1})[a]	0.023 × V_{cmax25}	(Launiainen et al., 2015)
Co-limitation parameter	0.95	
Curvature of electron transport light response (-)	0.7	(Launiainen et al., 2015)
Quantum yield parameter (mol mol^{-1})	0.2	(Launiainen et al., 2015)
Stomatal model slope (-)[b]	g_1	see Table 2
Residual conductance (mol m^{-2} s^{-1})[b]	g_0	see Table 2
Bryophyte layer parameters		
Height (m)	0.095	(Soudzilovskaia et al., 2013)
Roughness height (m)	0.01	(Launiainen et al., 2015)
Bulk density (kg m^{-3})	17.1	(Soudzilovskaia et al., 2013)
Total pore volume (m^3 m^{-3})	0.98	(Voortman et al., 2014)
Maximum gravimetric water content, w_{max} (g g^{-1})	10	(Soudzilovskaia et al., 2013)
Minimum gravimetric water content (g g^{-1})	1.5	(Launiainen et al., 2015)
Van Genuchten water retention parameter (cm^{-1})	0.13	(Voortman et al., 2014)
Van Genuchten water retention parameter (-)	2.17	(Voortman et al., 2014)
Saturated hydraulic conductivity (m/h)	4.2 × 10^{-4}	(Voortman et al., 2014)

Pore connectivity (-)	-2.37	(Voortman et al., 2014)
Emissivity (-)	0.98	(Campbell and Norman, 1998)
PAR albedo at w_{max} (-)[c]	0.11	(Bubier et al., 1997)
NIR albedo at w_{max} (-)[c]	0.29	(Bubier et al., 1997)
Top soil layer parameters		
Depth (m)	0.1	2 × measurement depth of soil temperature and moisture
Porosity (m^3/m^3)	0.8	(Launiainen et al., 2015)
Residual water content (m^3/m^3)	0.01	(Launiainen et al., 2015)
Van Genuchten water retention parameter (cm^{-1})	0.7	(Launiainen et al., 2015)
Van Genuchten water retention parameter (-)	1.25	(Launiainen et al., 2015)
Saturated hydraulic conductivity (m/h)	0.015	(Launiainen et al., 2015)
Thermal conductivity of solids (W/m/K)	2.17	Derived from soil composition[d]
Heat capacity of solids ($MJ/m^3/K$)	2.35	Derived from soil composition[d]

[a] Temperature response curves of V_{cmax} and J_{max} are apodted from Kattge and Knorr (2007) and of r_d from Launiainen et al. (2015)

[b] Parameters of Medlyn et al. (2011) optimal stomatal conductance model

[c] Response of albedo to bryophyte water content (Kieloaho and Launianen, 2018)

[d] Soil composition of top soil layer adopted from Jauhiainen (2004) and thermal properties soil materials from Tian et al. (2016) and Campbell and Norman (1998)

Table S2. Plant type specific model parameter values applied in simulations.

Description	Parameter value			
	Spruce	**Pine**	**Birch**	**Understory**
Maximum LAI, LAI_{max} (m^2/m^2)[a]	$0.31 \times LAI_{tot}$	$0.64 \times LAI_{tot}$	$0.05 \times LAI_{tot}$	0.4–0.8
Minimum LAI (m^2/m^2)[a]	$0.8 \times LAI_{max}$	$0.8 \times LAI_{max}$	$0.1 \times LAI_{max}$	$0.5 \times LAI_{max}$
Minimum value for seasonal cycle modifier (-)[b]	0.1	0.1	0.01	0.01
Characteristic leaf length scale (m)	0.02	0.02	0.05	0.05
Nitrogen attenuation coefficient (-)	0.5	0.5	0.2	0
V_{cmax25} (µmol m^{-2} s^{-1})	60	50	45	40
Stomatal model slope g_1 (-)	2.5	2.5	4.5	4.5
Residual conductance g_0 (mol m^{-2} s^{-1})	0.004	0.004	0.01	0.01

[a] Seasonal development of LAI starts when the degree day sum (T_{base} = 5°C) exceeds 45 days and reaches maturation at 250 days. Leaf senescence in autumn follows Launiainen et al. (2015). LAI_{tot} = 3.4–6.9 m^2 m^{-2}.

[b] Seasonal cycle modifier for photosynthetic capacity is based on the delayed effect of temperature (Kolari et al., 2007; Launiainen et al., 2015).

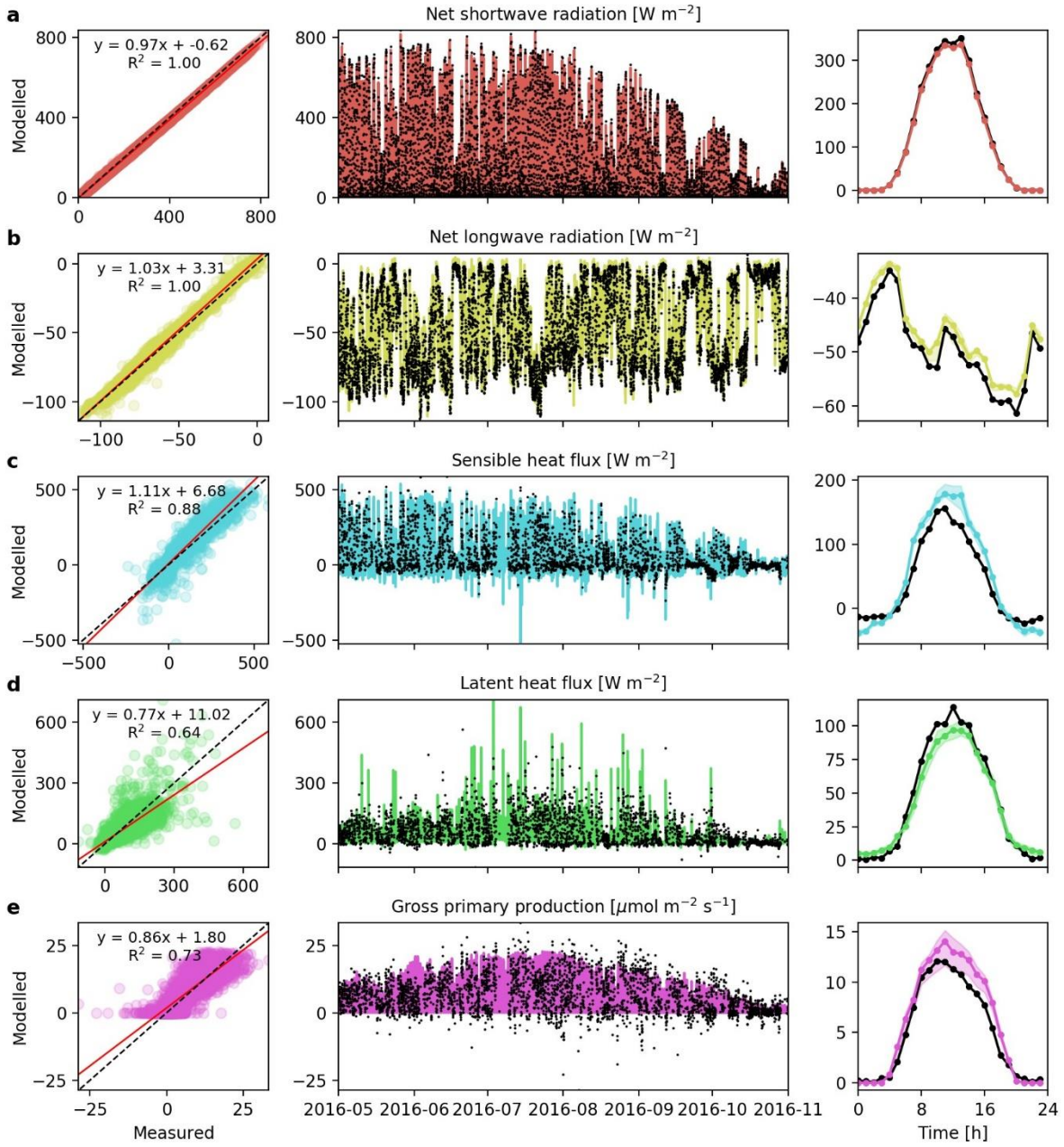

Figure S4. Scatter plot comparison, time series and average diurnal cycle for measured and modelled components of net radiation (a-b), sensible heat flux (c), latent heat flux (d), and gross primary production (e). Eddy covariance data (c-e) is non-gapfilled and only model results of times with data available are plotted in diurnal cycles. Modeled data are in colors and measured in black.

References

Bubier, J.L., Rock, B.N., Crill, P.M., 1997. Spectral reflectance measurements of boreal wetland and forest mosses. Journal of Geophysical Research: Atmospheres 102, 29483–29494. https://doi.org/10.1029/97JD02316

Campbell, G.S., Norman, J.M., 1998. Introduction to Environmental Biophysics, 2nd ed. Springer.

Jauhiainen, M., 2004. Relationships of particle size distribution curve, soil water retention curve and unsaturated hydraulic conductivity and their implications on water balance of forested and agricultural hillslopes. Helsinki University of Technology.

Kattge, J., Knorr, W., 2007. Temperature acclimation in a biochemical model of photosynthesis: a reanalysis of data from 36 species. Plant Cell Environ. 30, 1176–1190. https://doi.org/10.1111/j.1365-3040.2007.01690.x

Kieloaho, A.-J., Launianen, S., 2018. Effects of functional traits of bryophyte layer on water cycling and energy balance in boreal and arctic ecosystems, in: EGU General Assembly Conference Abstracts. p. 11786.

Kolari, P., Lappalainen, H.K., Hänninen, H., Hari, P., 2007. Relationship between temperature and the seasonal course of photosynthesis in Scots pine at northern timberline and in southern boreal zone. Tellus Series B-Chemical and Physical Meteorology 59, 542–552.

Launiainen, S., Katul, G.G., Lauren, A., Kolari, P., 2015. Coupling boreal forest CO2, H2O and energy flows by a vertically structured forest canopy – Soil model with separate bryophyte layer. Ecological Modelling 312, 385–405. https://doi.org/10.1016/j.ecolmodel.2015.06.007

Lee, X., Shaw, R.H., Black, T.A., 1994. Modelling the effect of mean pressure gradient on the mean flow within forests. Agricultural and Forest Meteorology 68, 201–212. https://doi.org/10.1016/0168-1923(94)90036-1

Medlyn, B.E., Duursma, R.A., Eamus, D., Ellsworth, D.S., Prentice, I.C., Barton, C.V.M., Crous, K.Y., Angelis, P.D., Freeman, M., Wingate, L., 2011. Reconciling the optimal and empirical approaches to modelling stomatal conductance. Global Change Biology 17, 2134–2144. https://doi.org/10.1111/j.1365-2486.2010.02375.x

Soudzilovskaia, N.A., van Bodegom, P.M., Cornelissen, J.H., 2013. Dominant bryophyte control over high-latitude soil temperature fluctuations predicted by heat transfer traits, field moisture regime and laws of thermal insulation. Functional Ecology 27, 1442–1454.

Stenberg, P., 1996. Correcting LAI-2000 estimates for the clumping of needles in shoots of conifers. Agricultural and Forest Meteorology 79, 1–8. https://doi.org/10.1016/0168-1923(95)02274-0

Tian, Z., Lu, Y., Horton, R., Ren, T., 2016. A simplified de Vries-based model to estimate thermal conductivity of unfrozen and frozen soil. European Journal of Soil Science 67, 564–572. https://doi.org/10.1111/ejss.12366

Voortman, B.R., Bartholomeus, R.P., Bodegom, P.M. van, Gooren, H., Zee, S.E.A.T.M. van der, Witte, J.-P.M., 2014. Unsaturated hydraulic properties of xerophilous mosses: towards implementation of moss covered soils in hydrological models. Hydrological Processes 28, 6251–6264. https://doi.org/10.1002/hyp.10111

Watanabe, T., Mizutani, K., 1996. Model study on micrometeorological aspects of rainfall interception over an evergreen broad-leaved forest. Agricultural and Forest Meteorology 80, 195–214. https://doi.org/10.1016/0168-1923(95)02301-1